Joint TX/RX IQ Mismatch Compensation Based on a Low-IF Internal Feedback Architecture

Chun-Hsien Peng † and Paul Liang †
† MediaTek Inc., Hsinchu, Taiwan, R.O.C.
Email: {ch.peng, paul.liang, hc.hwang}@mediatek.com

Charles Chien ‡, Bala Narasimhan ‡, and HC Hwang †
‡ MediaTek Inc., 2860 Junction Ave, San Jose, CA 95134, USA
Email: {charles.chien, bala.narasimhan}@mediatek.com

***Abstract*—Modern radios use in-phase (I) and quadrature-phase (Q) channels for transmission and reception. However, IQ matching for high image rejection ratio is difficult and costly to realize by pure analog circuit techniques. Therefore, digital-assisted IQ compensation is required. This paper presents a novel joint TX/RX IQ compensation (JTRC) algorithm for low-IF feedback architecture. Conventional approaches are based on time-domain processing of test tones or frequency-domain processing of pilots in orthogonal frequency-division multiplexing (OFDM) systems. In contrast, JTRC employs time-domain blind source separation (BSS) for both OFDM and non-OFDM based systems without placing a specific requirement on the type of test signal. For example, JTRC supports both tones and modulated signals. Moreover, JTRC can be performed in the background during normal transmission mode using the actual transmitted signal. Unlike other BSS approaches that can only compensate for RX IQ mismatches while assuming a matched transmitter, JTRC can jointly compensate for both TX and RX IQ mismatches. We present an in-depth analysis that validates the JTRC algorithm and show simulation results that demonstrate its effectiveness.**

I. Introduction

Analog components such as mixers and filters exhibit IQ mismatches due to asymmetry in devices and layouts. The IQ mismatches produces an image signal that distorts the desired signal and therefore degrades the performance of a communication system [1]–[4]. Such degradation is measured in terms of the image rejection ratio (IRR), defined as the ratio of the desired signal power to the image power in units of dB. An IRR of 40 dB or greater is usually needed to support high order constellation such as 256 quadrature amplitude modulation (QAM). To achieve such a high IRR, compensation of the IQ mismatches is necessary. Traditionally, tone-based IQ compensation algorithms have been used [1]. However, these algorithms cannot support background compensation during normal transmit or receive operation as the IQ mismatch changes with temperature and aging [2].

Valkama *et al* [3] proposed a blind source separation (BSS) algorithm under the assumption of a circular or proper signal. This algorithm has been applied to receiver (RX) IQ compensation using perfectly matched modulated signals received from a remote transmitter (TX), such as a basestation. However, perfect matching can never be achieved in practice. Transmitters do exhibit IQ mismatches, which can degrade the performance of the RX IQ compensator, especially, for high target IRR. Furthermore, their approach in using ensemble averaging to evaluate the performance of the compensation algorithm does not apply for receivers using an intermediate frequency (IF).

Recently, B. Debaillie *et al* [2] reported a compensation algorithm for orthogonal frequency-division multiplexing (OFDM) based systems such as WiMAX, Wi-Fi, and DVB-T/H. The algorithm utilizes a known preamble to estimate the TX/RX IQ mismatches in the frequency domain based on a low-IF internal feedback compensation (LIFC) architecture. However, this algorithm cannot be applied to non-OFDM based systems such as GSM, CDMA, and Bluetooth.

In this paper, we propose a novel joint TX/RX IQ compensation (JTRC) algorithm using BSS and test signals sent in an internal feedback path to estimate correction factors. Our approach applies to not only OFDM based systems but also non-OFDM based systems. Moreover, our algorithm supports the calibration for both the standby mode and normal transmit mode. In standby mode, tone signals can be used to shorten the convergence time. In transmit mode, actual transmitted signal is used to update the IQ compensation without interruption of normal operation. The JTRC algorithm provides an efficient correction mechanism for permutation ambiguity and scaling factor required when employing BSS. Because the JTRC algorithm processes a low-IF signal in the feedback path, it cannot be analyzed using traditional ensemble average techniques. Instead, we present an analysis based on time averaging that validates the effectiveness of JTRC algorithm in achieving high IRR required for high order modulation (e.g. 256 QAM), used in emerging systems such as IEEE 802.11ac.

II. Discrete-Time Signal Model

In this section, we present the signal model based on a low-IF feedback architecture as shown in Fig. 1. For ease of reference in later sections, we define the following notations:

$E\{\cdot\}$: expectation operator
$\langle \cdot \rangle$: time average operator
$\mathbf{I}$: 2×2 identity matrix
Superscript '$*$' : complex conjugation
Superscript 'T' : transpose of vectors or matrices
Superscript 'H': Hermitian of vectors or matrices
$\mathbf{H}_z$: 2×2 conjugate mixing matrix as

$$\mathbf{H}_z = \begin{pmatrix} \mathbf{h}_{z,1}^{\mathrm{T}} \\ \mathbf{h}_{z,2}^{\mathrm{T}} \end{pmatrix} \tag{1}$$

where $\mathbf{h}_{z,1} = (A_z, B_z)^{\mathrm{T}}$ and $\mathbf{h}_{z,2} = (B_z^*, A_z^*)^{\mathrm{T}}$.

978-1-4673-1881-5/12/$31.00 ©2012 IEEE

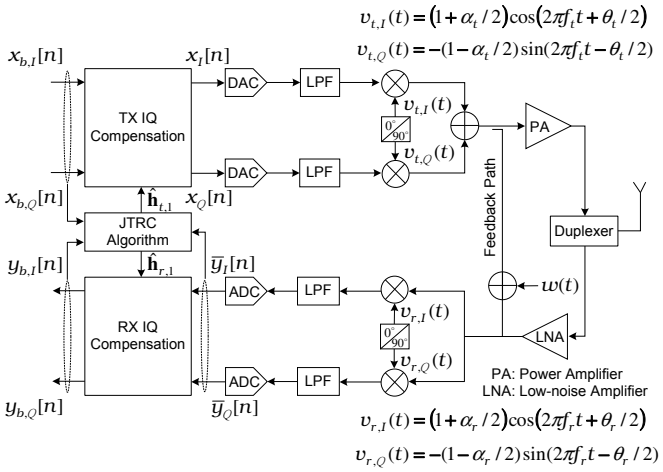

Fig. 1. The LIFC architecture with TX/RX IQ mismatches.

Consider a transceiver with IQ mismatches shown in Fig. 1 where $(\alpha_t,\ \theta_t)$ and $(\alpha_r,\ \theta_r)$ denote the gain and phase mismatch parameters of the TX and RX, respectively. Let $x[n] = x_I[n] + jx_Q[n]$ and $\bar{y}[n] = \bar{y}_I[n] + j\bar{y}_Q[n]$ be the input of the TX digital-to-analog converters (DACs) and output of the RX analog-to-digital converters (ADCs), respectively. Under the assumptions of frequency independent mismatches and that the sampling rates F_s of the ADC's and DAC's satisfy Nyquist criterion, the discrete-time signal $\bar{y}[n]$ can be expressed in terms of the gain and phase mismatches associated with the RX as shown below:

$$\bar{y}[n] = A_r y[n] + B_r y^*[n], \quad n = 0, 1, ..., N-1 \tag{2}$$

where N denotes data length and

$$A_r = (1/4)\left[(1-\alpha_r/2)e^{j\theta_r/2} + (1+\alpha_r/2)e^{-j\theta_r/2}\right] \tag{3}$$

$$B_r = (1/4)\left[(1+\alpha_r/2)e^{j\theta_r/2} - (1-\alpha_r/2)e^{-j\theta_r/2}\right]. \tag{4}$$

Let f_t and f_r be the TX and RX carrier frequencies, respectively. In (2), $y[n]$ can be further expressed in terms of the gain and phase mismatches associated with the TX as follows:

$$y[n] = (\bar{x}[n] + w[n])\, e^{j2\pi f_I n/F_s} \tag{5}$$

where $f_I = f_t - f_r$ denotes low-IF frequency, $w[n]$ is a discrete-time noise signal, and

$$\bar{x}[n] = A_t x[n] + B_t x^*[n]. \tag{6}$$

The coefficients A_t and B_t can be expressed as follows

$$A_t = (1/2)\left[(1+\alpha_t/2)e^{j\theta_t/2} + (1-\alpha_t/2)e^{-j\theta_t/2}\right] \tag{7}$$

$$B_t = (1/2)\left[(1+\alpha_t/2)e^{j\theta_t/2} - (1-\alpha_t/2)e^{-j\theta_t/2}\right]. \tag{8}$$

III. Brief Review of the BSS Algorithm in a Conjugate Signal Model

Consider a conjugate signal model shown in [3] defined as

$$\mathbf{o}[n] = (o_1[n], o_2[n])^{\mathrm{T}} = \mathbf{H_o}\mathbf{s}[n] + \mathbf{w}[n], \tag{9}$$

where $o_2^*[n] = o_1[n]$, $\mathbf{H_o}$ is an unknown conjugate mixing matrix (see (1), subscript "z" replaced by "$\mathbf{o}$"), $\mathbf{s}[n] = (s_1[n], s_2[n])^{\mathrm{T}} = (s[n], s^*[n])^{\mathrm{T}}$ are the input sources, and $\mathbf{w}[n]$ is a noise vector. Next, let us briefly review how to separate the two sources, $s_1[n]$ and $s_2[n]$, with an unknown $\mathbf{H_o}$ under the following assumption:

(A1) The signals $s[n]$ and $s^*[n]$ are circular or proper signals, i.e. $E\{s^2[n]\} = E\{(s^*[n])^2\} = 0$.

By (A1) and under a noise-free assumption, Valkama *et al.* [3] show that a 2×2 separation matrix $\widetilde{\mathbf{H}}_{\mathbf{o}}$ can be found using eigenvalue decomposition (EVD) of the correlation matrix of $\mathbf{o}[n]$ as shown below:

$$\mathbf{C_o} = E\{\mathbf{o}[n]\mathbf{o}^{\mathrm{H}}[n]\} = \sigma_s^2 \mathbf{H_o}\mathbf{H_o}^{\mathrm{H}}, \tag{10}$$

where $\sigma_s^2 = E\{|s[n]|^2\}$. Then, it's outputs $\widetilde{\mathbf{o}}[n] = (\widetilde{o}_1[n], \widetilde{o}_2[n])^{\mathrm{T}} = \widetilde{\mathbf{H}}_{\mathbf{o}}\mathbf{o}[n] = \widetilde{\mathbf{H}}_{\mathbf{o}}\mathbf{H_o}\mathbf{s}[n]$, where $\widetilde{o}_1[n]$ could be equal to either $\alpha s_1[n]$ or $\beta s_2[n]$ and $\widetilde{o}_2^*[n] = \widetilde{o}_1[n]$. The fact that $\widetilde{o}_1[n]$ could be a scaled version of either $s_1[n]$ or $s_2[n]$ is referred to as permutation ambiguity with an unknown complex scale factor α or β.

A remark about the existing BSS algorithm is as follows:

(R1) Under the assumption of a circular or proper signal using ensemble average, [3] shows that we can find a separation matrix with the permutation ambiguity and unknown complex scale factor. Usually, the permutation ambiguity can be corrected by the use of side information such as pilots sent from a basestation. The unknown complex scale factor can be estimated and corrected by phase synchronization or channel estimation/equalization. However, [3] can only be applied to RX IQ compensation due to its assumption on a matched transmitted signal.

IV. Proposed JTRC Algorithm

First, a tone-based or modulated source, $x_b[n] = x_{b,I}[n] + jx_{b,Q}[n]$, is transmitted and looped back to the RX as shown in Fig. 1. The received data, $\bar{y}[n]$, is then stored. The same data is used for the joint estimation of RX and TX IQ compensators denoted by $\widehat{\mathbf{h}}_{r,1} = (\widehat{h}_{r,1}, \widehat{h}_{r,2})^{\mathrm{T}}$ and $\widehat{\mathbf{h}}_{t,1} = (\widehat{h}_{t,1}, \widehat{h}_{t,2})^{\mathrm{T}}$, respectively.

The conjugate signal model described in Section III will be used to analyze the JTRC algorithm. To obtain a conjugate signal model representation, the two signals $\bar{y}[n]$ and $\bar{y}^*[n]$ given by (2) are grouped into a vector $\bar{\mathbf{y}}[n]$ as shown below:

$$\bar{\mathbf{y}}[n] = (\bar{y}[n], \bar{y}^*[n])^{\mathrm{T}} = \mathbf{H}_r\mathbf{y}[n] \tag{11}$$

where $\mathbf{y}[n] = (y[n], y^*[n])^{\mathrm{T}}$ and $\mathbf{H}_r$ is a conjugate mixing matrix defined in (1) with subscript "z" replaced by "r". In $\mathbf{H}_r$, A_r and B_r are defined respectively in (3) and (4). Before describing the algorithm to estimate $\widehat{\mathbf{h}}_{r,1}$ and $\widehat{\mathbf{h}}_{t,1}$, we define the IRRs [2], [3] for TX and RX, respectively.

For the RX, the output of the RX IQ compensator $\widehat{\mathbf{h}}_{r,1}$ can be expressed by

$$y_b[n] = y_{b,I}[n] + jy_{b,Q}[n] = \widehat{\mathbf{h}}_{r,1}^{\mathrm{T}}\bar{\mathbf{y}}[n] = \mathbf{g}_r^{\mathrm{T}}\mathbf{y}[n] \tag{12}$$

where $\mathbf{y}[n]$ is given by (11) and $\mathbf{g}_r = (g_{r,1}, g_{r,2})^{\mathrm{T}} = \mathbf{H}_r^{\mathrm{T}} \widehat{\mathbf{h}}_{r,1}$ denotes the overall gains associated with the wanted signal and undesired image. For the TX, the output of the compensator $\widehat{\mathbf{h}}_{t,1}$ can be expressed as

$$x[n] = \widehat{\mathbf{h}}_{t,1}^{\mathrm{T}} \mathbf{x}_b[n] \tag{13}$$

where $\mathbf{x}_b[n] = (x_b[n], x_b^*[n])^{\mathrm{T}}$. Next, according to (6), the baseband equivalent output signal from the TX mixers can be expressed as follows

$$\bar{x}[n] = \mathbf{g}_t^{\mathrm{T}} \mathbf{x}_b[n] \tag{14}$$

where the overall gains $\mathbf{g}_t = (g_{t,1}, g_{t,2})^{\mathrm{T}} = \widehat{\mathbf{H}}_t^{\mathrm{T}} \mathbf{h}_{t,1}$ in which $\mathbf{h}_{t,1} = (A_t, B_t)^{\mathrm{T}}$ is the TX IQ mismatch vector defined in (6), (7), and (8), and

$$\widehat{\mathbf{H}}_t = \begin{pmatrix} \widehat{\mathbf{h}}_{t,1}^{\mathrm{T}} \\ \widehat{\mathbf{h}}_{t,2}^{\mathrm{T}} \end{pmatrix}. \tag{15}$$

In (15), the $\widehat{\mathbf{h}}_{t,2} = (\widehat{h}_{t,2}^*, \widehat{h}_{t,1}^*)^{\mathrm{T}}$ is the conjugate form of $\widehat{\mathbf{h}}_{t,1}$. The IRRs for TX and RX can be defined respectively as

$$\mathrm{IRR}_{\mathrm{TX}} = 10\log_{10}\left(|g_{t,1}|^2/|g_{t,2}|^2\right) \quad (\mathrm{dB}) \tag{16}$$

$$\mathrm{IRR}_{\mathrm{RX}} = 10\log_{10}\left(|g_{r,1}|^2/|g_{r,2}|^2\right) \quad (\mathrm{dB}). \tag{17}$$

A remark about IRRs is as follows:

(R2) In practice, without IQ compensation (i.e., $\widehat{\mathbf{h}}_{t,1} = \widehat{\mathbf{h}}_{r,1} = (1,0)^{\mathrm{T}}$), the image attenuation is about 25-35 dB (i.e., $|A_r| \gg |B_r|$ and $|A_t| \gg |B_t|$) and is insufficient for wireless communication applications [4].

A. RX IQ Compensator ($\widehat{\mathbf{h}}_{r,1}$) Estimation

The estimation of RX IQ compensator $\widehat{\mathbf{h}}_{r,1}$ includes two steps: the first involves the estimation of the RX separation matrix and the second involves the correction of permutation ambiguity by a known training signal.

1) RX Separation Matrix Estimation: Consider a single-tone training signal defined as $x_b[n] = e^{j2\pi f_b n/F_s}$, where $f_b \neq 0$. At the beginning of the training, we let $\widehat{\mathbf{h}}_{t,1} = (1,0)^{\mathrm{T}}$ (i.e., $x[n] = x_b[n]$). We further define the signal used for RX permutation ambiguity correction as follows

$$\widetilde{x}_b[n] = x_b^*[n]\left(e^{j2\pi f_I n/F_s} + e^{-j2\pi f_I n/F_s}\right) \tag{18}$$

where the f_I and F_s are known in advance. Next, we define in **Lemma 1** on the derivation of time averages of key parameters needed for further analysis.

Lemma 1 (Single-tone Signal). Under a noise-free assumption, the following time averages converge to

$$\langle y^2[n]\rangle \longrightarrow \eta_y = \begin{cases} 0, & \text{for } f_I \neq 0, f_I \neq \pm f_b \\ 2A_tB_t, & \text{for } f_I = 0 \\ A_t^2, & \text{for } f_I = -f_b \\ B_t^2, & \text{for } f_I = f_b, \end{cases} \tag{19}$$

$$\langle (y^*[n])^2\rangle \longrightarrow \eta_y^*, \tag{20}$$

$$\langle y[n]\cdot \widetilde{x}_b[n]\rangle \longrightarrow A_t, \quad \text{for } f_I \neq f_b, f_I \neq 0, f_b \neq 0, \tag{21}$$

$$\langle y^*[n]\cdot \widetilde{x}_b[n]\rangle \longrightarrow B_t^*, \text{ for } f_I \neq -f_b, f_I \neq 0, f_b \neq 0, \tag{22}$$

where $\longrightarrow$ denotes "convergence" as the data length N in (2) approaches ∞.

Using (19) and (20) in **Lemma 1**, it can be shown that

$$\mathbf{C}_{\bar{\mathbf{y}}} = \langle \bar{\mathbf{y}}[n]\bar{\mathbf{y}}^{\mathrm{H}}[n]\rangle \longrightarrow \mathbf{H}_r \mathbf{K} \mathbf{H}_r^{\mathrm{H}} \tag{23}$$

where

$$\mathbf{K} = \begin{pmatrix} \sigma_y^2 & \eta_y \\ \eta_y^* & \sigma_y^2 \end{pmatrix} \tag{24}$$

in which $\sigma_y^2 = \langle |y[n]|^2\rangle \longrightarrow |A_t|^2 + |B_t|^2$ and η_y is given by (19). If $f_I \neq 0$ and $f_I \neq \pm f_b$, then $\eta_y = 0$, implying that $y[n]$ is a circular signal and $\mathbf{C}_{\bar{\mathbf{y}}} \longrightarrow \sigma_y^2 \mathbf{H}_r \mathbf{H}_r^{\mathrm{H}}$. Thus, as discussed in Section III, EVD can be applied to find a separation matrix:

$$\widetilde{\mathbf{H}}_r = \begin{pmatrix} \widetilde{\mathbf{h}}_{r,1}^{\mathrm{T}} \\ \widetilde{\mathbf{h}}_{r,2}^{\mathrm{T}} \end{pmatrix}, \tag{25}$$

where $\widetilde{\mathbf{h}}_{r,l}, l = 1,2$ are 2×1 vectors. According to (25) and (11), we have the output as follows:

$$\widetilde{\mathbf{y}}[n] = (\widetilde{y}_1[n], \widetilde{y}_2[n])^{\mathrm{T}} = \widetilde{\mathbf{H}}_r \bar{\mathbf{y}}[n] = \widetilde{\mathbf{H}}_r \mathbf{H}_r \mathbf{y}[n], \tag{26}$$

where $\widetilde{y}_2[n] = \widetilde{y}_1^*[n]$ and $\widetilde{y}_1[n] \longrightarrow \alpha_r y[n]$ or $\beta_r y^*[n]$ in which α_r and β_r are unknown complex scale factors.

Two remarks regarding $\widetilde{\mathbf{H}}_r$ are as follows:

(R3) Because $y[n]$ violates ergodicity (i.e., $E\{y^2[n]\} \neq \langle y^2[n]\rangle$ for $f_I \neq 0$ and $f_I \neq \pm f_b$), we used time averaging in **Lemma 1** instead of ensemble expectation to prove that the wanted signal and the unwanted image can be separated by BSS. This holds true even if $y[n]$ or $y^*[n]$ includes the wanted signal and image source of TX provided that $f_I \neq 0$.

(R4) Although the unknown scale factor α_r or β_r can be corrected by digital processing before the final data detection at the receiver, the permutation ambiguity issue still must be resolved (see (R1)).

2) Permutation Ambiguity Correction: The baseband signal $x_b[n]$, low-IF frequency f_I, and sampling rate F_s are known in advance. Therefore, based on (18), (21), (22), and $|A_t| \gg |B_t|$ (see (R2)), the RX compensator can be expressed as

$$\widehat{\mathbf{h}}_{r,1} = \widetilde{\mathbf{h}}_{r,L_r} \tag{27}$$

where $\widetilde{\mathbf{h}}_{r,l}$ is given by (25) and

$$L_r = \arg\max_l \left\{ |\langle \widetilde{y}_l[n]\cdot \widetilde{x}_b[n]\rangle|,\ l = 1,2 \right\}, \tag{28}$$

in which $\widetilde{y}_l[n]$ is given by (26). By substituting (27) into (12), the output signal of $\widehat{\mathbf{h}}_{r,1}$ with the permutation ambiguity correction is

$$y_b[n] = \widehat{\mathbf{h}}_{r,1}^{\mathrm{T}} \bar{\mathbf{y}}[n] = \mathbf{g}_r^{\mathrm{T}} \mathbf{y}[n] = \widetilde{y}_{L_r}[n] \longrightarrow \bar{\alpha}_r y[n] \tag{29}$$

where $\mathbf{g}_r = (\bar{\alpha}_r, 0)^{\mathrm{T}}$ and $\bar{\alpha}_r = \alpha_r$ or β_r.

B. TX IQ Compensator ($\widehat{\mathbf{h}}_{t,1}$) Estimation

After the RX IQ compensation, JTRC performs TX IQ compensation which includes the estimation of a separation matrix followed by the correction of unknown complex scale factor and permutation ambiguity.

1) TX separation matrix estimation: Because f_I is known in advance, after the RX IQ compensation we perform first a digital down-conversion shown below:

$$\bar{y}_b[n] = y_b[n] \cdot e^{-j2\pi f_I n/F_s}. \tag{30}$$

According to (29) and (5), $\bar{y}_b[n]$ can converge to $\bar{\alpha}_r \bar{x}[n]$ under noise-free condition. Next, by grouping the two signals $\bar{y}_b[n]$ and $\bar{y}_b^*[n]$ into a signal vector $\bar{\mathbf{y}}_b[n]$, and referring to (6), the following is obtained:

$$\bar{\mathbf{y}}_b[n] = (\bar{y}_b[n], \bar{y}_b^*[n])^{\mathrm{T}} \longrightarrow \Gamma \mathbf{H}_t \mathbf{x}[n], \tag{31}$$

where $\mathbf{x}[n] = (x[n], x^*[n])^{\mathrm{T}}$, $\mathbf{H}_t$ is a conjugate mixing matrix shown in (1) consisting of A_t and B_t, and $\Gamma = \mathrm{diag}\{\bar{\alpha}_r, \bar{\alpha}_r^*\}$ which is a diagonal matrix with elements $\bar{\alpha}_r$ and $\bar{\alpha}_r^*$. For single-tone signal $x[n] = x_b[n] = e^{j2\pi f_b n/F_s}$ with $\langle x^2[n] \rangle \longrightarrow 0$ when $f_b \neq 0$, the correlation matrix of $\bar{\mathbf{y}}_b[n]$ can be derived based on (31):

$$\mathbf{C}_{\bar{\mathbf{y}}_b} = \langle \bar{\mathbf{y}}_b[n] \bar{\mathbf{y}}_b^{\mathrm{H}}[n] \rangle \longrightarrow \sigma_x^2 \mathbf{G}_t \mathbf{G}_t^{\mathrm{H}} = \mathbf{G}_t \mathbf{G}_t^{\mathrm{H}}, \tag{32}$$

where $\sigma_x^2 = \langle |x[n]|^2 \rangle \longrightarrow 1$ and $\mathbf{G}_t = \Gamma \mathbf{H}_t$, which is also a conjugate mixing matrix.

Because (31) is a 2×2 conjugate model, EVD can be applied again to (32) to derive the TX separation matrix:

$$\widetilde{\mathbf{H}}_t = \begin{pmatrix} \widetilde{\mathbf{h}}_{t,1}^{\mathrm{T}} \\ \widetilde{\mathbf{h}}_{t,2}^{\mathrm{T}} \end{pmatrix}, \tag{33}$$

where $\widetilde{\mathbf{h}}_{t,l}, l = 1, 2$ are 2×1 vectors. By applying (33) to (31), the outputs of $\widetilde{\mathbf{H}}_t$ show permutation ambiguity as follows:

$$\widetilde{\mathbf{y}}_b[n] = (\widetilde{y}_{b,1}[n], \widetilde{y}_{b,2}[n])^{\mathrm{T}} = \widetilde{\mathbf{H}}_t \bar{\mathbf{y}}_b[n] \longrightarrow \widetilde{\mathbf{H}}_t \mathbf{G}_t \mathbf{x}[n], \tag{34}$$

where $\widetilde{y}_{b,2}[n] = \widetilde{y}_{b,1}^*[n]$ and $\widetilde{y}_{b,1}[n]$ converges to $\alpha_t x[n]$ or $\beta_t x^*[n]$ in which α_t and β_t are unknown complex scale factors. Note that $x[n] = x_b[n]$. In addition to permutation ambiguity correction, the α_t or β_t must also be determined by using the known $x_b[n]$ for the estimation of the $\widehat{\mathbf{h}}_t$ described below.

2) Scale Factor and Permutation Ambiguity Correction: Let

$$L_t = \arg\max_l \{|\widehat{\alpha}_{t,l}|, \ l = 1, \ 2\}, \tag{35}$$

where $\widehat{\alpha}_{t,l} = \langle \widetilde{y}_{b,l}[n] x_b^*[n] \rangle$ in which $\widetilde{y}_{b,l}[n]$ is given (34). It can be easily shown that $\widehat{\alpha}_{t,L_t} \longrightarrow \alpha_t$ or β_t^*. Thus, by applying (35) to (33), the following TX compensator is obtained:

$$\widehat{\mathbf{h}}_{t,1} = \frac{1}{\widehat{\alpha}_{t,L_t}} \widetilde{\mathbf{h}}_{t,L_t} \tag{36}$$

such that

$$\widehat{\mathbf{h}}_{t,1}^{\mathrm{T}} \bar{\mathbf{y}}_b[n] = \widehat{\mathbf{h}}_{t,1}^{\mathrm{T}} \mathbf{G}_t \mathbf{x}[n] \longrightarrow x[n] \quad (\text{see } (34)) \tag{37}$$

which, by inspection of (15) and (32), implies that

$$\widehat{\mathbf{H}}_t \mathbf{G}_t = \mathbf{I} = \mathbf{G}_t \widehat{\mathbf{H}}_t = \Gamma \mathbf{H}_t \widehat{\mathbf{H}}_t. \tag{38}$$

Thus, from (38), $\widehat{\mathbf{H}}_t^{\mathrm{T}} \mathbf{H}_t^{\mathrm{T}} = \mathrm{diag}\{1/\bar{\alpha}_r, 1/\bar{\alpha}_r^*\}$ which implies $\widehat{\mathbf{H}}_t^{\mathrm{T}} \mathbf{h}_{t,1} = \mathbf{g}_t = (1/\bar{\alpha}_r, 0)^{\mathrm{T}}$ and $\bar{x}[n] = (1/\bar{\alpha}_r) \cdot x_b[n]$ (see (14)). In other words, $\widehat{\mathbf{h}}_{t,1}$ can compensate the TX IQ mismatch $\mathbf{h}_{t,1}$.

Next, in addition to single-tone signals, the JTRC algorithm can also support modulated sources such as QAM sources as shown in Lemma below.

Lemma 2 (Modulated Signal). Under a noise-free assumption, it can be shown that time averages of the following statistics for modulated signals converge to definitive values shown in (39) - (42):

$$\langle y^2[n] \rangle \longrightarrow \eta_y = \begin{cases} 0, & \text{for } f_I \neq 0 \\ 2A_t B_t, & \text{for } f_I = 0, \end{cases} \tag{39}$$

$$\langle (y^*[n])^2 \rangle \longrightarrow \eta_y^*, \tag{40}$$

$$\langle y[n] \cdot \widetilde{x}_b[n] \rangle \longrightarrow A_t, \ \text{ for } f_I \neq 0 \tag{41}$$

$$\langle y^*[n] \cdot \widetilde{x}_b[n] \rangle \longrightarrow B_t^*, \ \text{ for } f_I \neq 0. \tag{42}$$

(R5) According to **Lemma 2**, $y[n]$ can be treated as a circular signal when $f_I \neq 0$. Under this condition, $\mathbf{K}$ in (24) converges to $\sigma_y^2 \mathbf{I}$ such that a separation matrix $\widetilde{\mathbf{H}}_r$ can be found by EVD as shown in the derivations (23) through (25). Therefore, the JTRC algorithm can also be applied to any modulated sources provided that the sources are circular and $f_I \neq 0$.

V. Simulation Results

Consider a transceiver with TX IRR of 29 dB and RX IRR of 25 dB, respectively, before compensation. Simulations are performed using QAM sources and a single-tone source with $f_b = 1$ MHz and $F_s = 40$ MHz. One hundred independent runs are performed for each simulation result. Signal-to-noise ratio (SNR) is defined as $\mathrm{SNR} = 1/\sigma_w^2$ where $\sigma_w^2 = E\{|w[n]|^2\}$ denotes the noise power of $w[n]$, a zero-mean Gaussian noise.

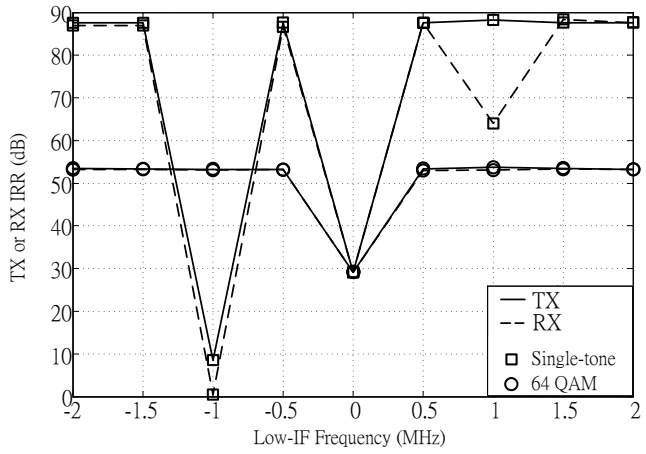

Fig. 2. Simulated IRRs versus f_I for SNR=40 dB and N=40000 achieved by the JTRC algorithm with single-tone and 64 QAM.

Fig. 2 shows IRRs versus low-IF frequency f_I for SNR=40 dB and the data length N=40000 for single-tone and 64 QAM. The IRR curves show that JTRC achieves greater than 80 dB for single-tone sources and 50 dB for 64 QAM sources, consistent with (R3) and (R5), respectively. In addition to SNR

and N, the performance of JTRC depends on η_y given in (19) and (39) defined for single-tone and modulated signals. By (24), as $|\eta_y|$ decreases, $\mathbf{K}$ approaches $\sigma_y^2\mathbf{I}$, resulting in larger IRR. The results in Fig. 2 for a single-tone validates **Lemma 1**, by which it is expected that the performance for $f_I = 1$ MHz ($\eta_y = B_t^2$) exceeds that of $f_I = 0$ MHz ($\eta_y = 2A_tB_t^2$) and $f_I = -1$ MHz ($\eta_y = A_t^2$) because $|A_t| \gg |B_t|$. Moreover, the performance for single-tone sources exceeds that of 64 QAM sources for $N = 40000$. This is because longer time is required for $|\langle y^2[n]\rangle|$ to reach zero when $f_I \neq 0$.

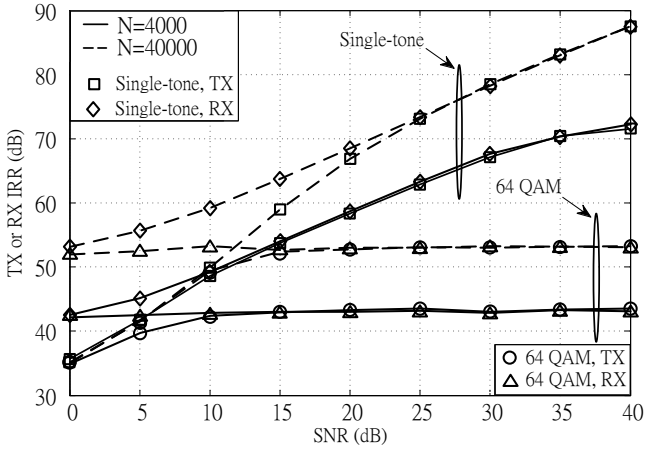

Fig. 3. Simulated IRRs versus SNR for different N and $f_I = 2$ MHz achieved by the JTRC algorithm with single-tone and 64 QAM.

Fig. 3 shows TX and RX IRRs versus SNR for single-tone and 64 QAM calibration sources. It is evident that the IRR performance of JTRC is increased as N increases because a larger N leads to a smaller $|\langle y^2[n]\rangle|$. One can see that IRR's greater than 40 dB can be achieved for SNR > 15 dB. In practice, such IRR is sufficient for current wireless systems applications such as Bluetooth or Wi-Fi. Moreover, the short sample length enables JTRC to achieve a high IRR with a short compensation time of 0.1ms ($4000/(40 \cdot 10^6)$) for single-tone sources which helps to reduce system overhead.

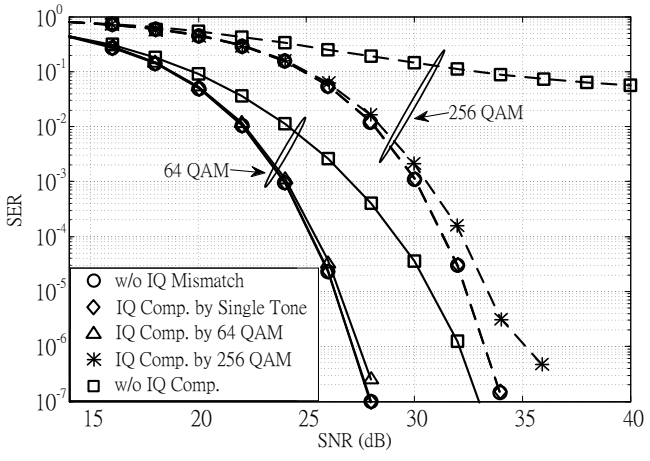

Fig. 4. Simulated SER versus SNR for $N = 4000$ and $f_I = 2$ MHz achieved by the JTRC algorithm with single-tone, 64 QAM, and 256 QAM.

Fig. 4 shows the symbol error rate (SER) versus SNR after IQ compensation by the JTRC algorithm with single-tone and modulated signals such as QAM. For 64 QAM, the SER performance with IQ compensation using single-tone (♢) or 64 QAM (△) is almost identical to that without any IQ mismatch (◯). In this case, JTRC regains the 4 dB SNR loss in the absence of compensation (□). As expected, the degradation is more severe for 256 QAM. In this case, the SER of 256 QAM is unacceptably high even with increasing SNR due to the error floor caused by the distortion from IQ mismatch. At an SER of 10^{-3}, JTRC algorithm using single-tone (♢) or 256 QAM ($*$) effectively mitigates the SNR degradation to less than 0.5 dB, a dramatic improvement for 256 QAM. If even more improvement is desired, the data length N can be increased to achieve higher IRR to further reduce the SNR loss below 0.5 dB.

VI. Conclusion

We have presented a novel joint TX/RX IQ compensation (JTRC) algorithm based on a low-IF feedback architecture using BSS. JTRC is waveform independent and can be applied to both OFDM and non-OFDM based systems. Unlike other BSS-based algorithms, JTRC can compensate for not only the RX mismatches but also TX mismatches jointly. We have presented theoretical analysis based on time average rather than ensemble average to validate the algorithm. Simulation results show that JTRC can converge in less than 0.1ms for tone-based signal and less than 1ms for modulated signal. The short convergence time using tones reduces the system overhead during periodic wake-up and the use of modulated signal enables seamless tracking of compensation vectors during normal transmission mode. Simulation results also show that IRR in excess of 60-75 dB and 42-52 dB can be achieved, respectively, for a single tone and a QPSK source. SER simulation shows that such high IRR is more than sufficient to support existing systems such as IEEE 802.11a/g/n and emerging systems such as IEEE 802.11ac that requires high order modulation (e.g. 256 QAM). Finally, it should be noted that the JTRC algorithm relies on a low-IF carrier only during calibration. During normal operation, the computed compensation vectors can improve the IRR performance of both a low-IF and a direct-conversion transceiver, making this algorithm attractive for a broad range of transceiver designs.

References

[1] S. Burglechner, G. Hueber, and A. Springer, "On the estimation and compensation of IQ impairments in direct conversion transmitters," *in Proc. IEEE EuWit 2008*, Oct. 27–28, 2008, pp. 69–72.

[2] B. Debaillie, P. Van Wesemael, G. Vandersteen, and J. Craninckx, "Calibration of Direct-Conversion Transceivers," *IEEE Journal of Selected Topics in Signal Processing*, vol. 3, no. 3, pp. 488–498, June 2009.

[3] M. Valkama, M. Renfors, and V. Koivunen, "Blind signal estimation in conjugate signal models with application to I/Q imbalance compensation," *IEEE Signal Processing Letters,* vol. 12, no. 11, pp. 733–736, Nov. 2005.

[4] M. Valkama, M. Renfors, and V. Koivunen, "Advanced methods for I/Q imbalance compensation in communication receivers," *IEEE Trans. Signal Processing,* vol. 49, no. 10, pp. 2335–2344, Oct. 2001.